CHALMERS

UNIVERSITY OF TECHNOLOGY

Doppler Shift Estimation for Intelligent Beamweight Computation

Ermias Habtegebriel

Doppler Shift Estimation for Intelligent Beam Weight Computation

Ermias Habtegebriel

Chalmers University of Technology
Department of Electrical Engineering
SE-412 96 Gothenburg
Sweden Telephone +46 76 560 5896

Abstract

Estimation of the Doppler frequency plays an important role by providing information on how to use the channel resources effectively. This thesis work analyses the various alternatives for Doppler estimation in the up link of an LTE beamforming system on a MATLAB simulation environment. Various methods are compared in terms of complexity, performance under noise, estimation range, and accuracy. Specifically, the pilot based and cyclic prefix methods are investigated and comparisons are made in three propagation channel models namely the extended pedestrian A model, the extended vehicular A model, and extended Typical Urban model. It is shown that except for the estimation range, the pilot method shows superior performance over the cyclic prefix method. Furthermore, the result of the estimation is used in optimizing the performances of the LTE system and high performance gain is observed in the extended pedestrian channel.

Acknowledgements

I would like to thank Erik Dahlbäck , Harish Venkatraman Bhat, and Johan Åman who gave me the opportunity to do this Master's thesis at Ericsson and who also provided me with valuable support during the work. I would also like to thank Professor Henk Wymeersch and Li Yan at Chalmers University of Technology for their guidance throughout this thesis work. Finally a big thanks to family and friends who have supported me during my studies.

<div align="right">

Ermias Habtegebriel, Gothenburg, 2017

</div>

Contents

List of Figures

List of Tables

Acronym

ACF Auto Correlation Function
AWGN Additive White Gaussian Noise
BER Bit Error Rate
BLER Block Error Rate

CSI Channel State Information
CRC Cyclic Redundancy Check
CSI-RS Channel State Information Reference Signals
CRS Cell Specific Reference Signals

DL Downlink
DMRS Demodulation Reference Signal

eNB Evolved Node B
EPA Extended Pedestrian A model
ETU Extended Typical Urban model
E-UTRA Enhanced-Universal Terrestrial Radio Access
EVA Extended Vehicular A model

FDD Frequency Division Duplex
FFT Fast Fourier Transform
HST High Speed Train
ICI Inter Carrier Interference
IFFT Inverse Fast Fourier Transform
ISI Inter Symbol Interference

LCR Level Crossing Rate
LTE Long Term Evolution

MBSFN Multicast Broadcast Single Frequency Network
MCH Multicast Channel
MIB Master Information Block
MIMO Multiple Input Multiple Output
MRT Maximum Ratio Transmission
MUI Multi User Interference
MU-MIMO Multi User Multiple Input Multiple Output
MU-SIMO Multi User Single Input Multiple Output

OFDM Orthogonal Frequency Division Multiplexing
OFDMA Orthogonal Frequency Division Multiple Access

PAPR Peak to Average Power Ratio
PBCH Physical Broadcast Channel
PCFICH Physical Control Format Indicator Channel

PDCCH Physical Downlink Control Channel
PDSCH Physical Downlink Shared Channel
PUSCH Physical Uplink Shared Channel

QAM Quadrature Amplitude Modulation
QPSK Quadrature Phase Shift Keying

RB Resource Block
RZF Reduced Zero Forcing

SC-FDMA Single Carrier Frequency Division Multiple Access
SDMA Space Division Multiple Access
SNR Signal to Noise Ratio
SRS Sounding Reference Signal
SDMA Space Division Multiple Access

TDD Time Division Duplex

UE User Equipment
UP Uplink

ZF Zero Forcing

1

Introduction

The ever growing demand of high data rates has lead to the developments of the long term evolution (LTE) system. LTE has several advantages such as high data rates, low latency, and time division duplex (TDD) and frequency division duplex (FDD) on the same platform. In order to achieve the advantages mentioned above a technique called beamforming, which is used for directional signal transmission, improved signal to noise ratio (SNR), reduced interference, and higher capacity, has been proposed.

1.1   Motivation

In LTE beamforming systems, there is an enormous amount of complexity involved in computing the beamforing weights. The weights has to be computed for each user and base station antenna and this makes the computation a very demanding task.

One way of reducing the complexity is by reusing the beamweights for a number of downlink transmissions based on the channel condition,i.e., how fast the channel is changing, and Doppler frequency is one of the most important parameters providing this information.

1.2   Objectives

This thesis work aims to study doppler shift estimation in an LTE system. Various methods will be investigated and compared based on four criterias namely complexity, performance under noise, accuracy, and estimation range. The algorithm which shows superior performance will be used to optimize the system by reducing the complexity in different channel conditions. The work will be done based on a reference set up shown in Figure 1.1.

Transmitter Block

Bits — QAM modulation — Layer mapping — Precoding — OFDMA/SCFDMA

Receiver Block

Rx — OFDMA/SCFDMA — Channel Estimation — Channel equalization

Symbol Demodulation — Layer Demapping
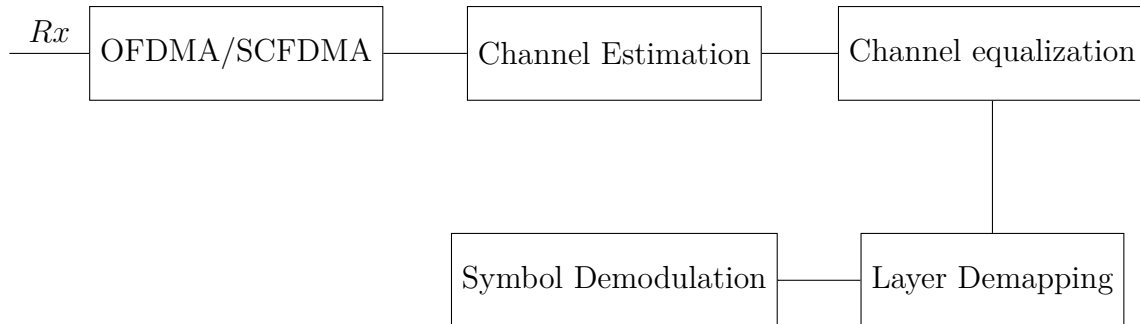
Figure 1.1: Block diagram of the reference system

The outcome of the thesis will be important in adding a better understanding of LTE beamforming systems. In addition, the result could be used in areas which require doppler estimation as an input.

1.3 Methodology

In order to achieve the objectives stated above, the following steps will be followed:

1. Literature study

   The thesis work will begin by a brief literature study on the effect of doppler shift on the performance of a wireless system and the various methods of estimating the shift. In addition, the study will also include a brief revision of the LTE standards and beamforming techniques.

2. Comparing the various Doppler shift estimation algorithms

   The purpose of this stage is to extensively study the current research and analyse the various alternatives for doppler estimation. The methods will be compared in terms of four parameters: complexity, performance under noise, accuracy, and estimation range

3. Implementation of the algorithms

   After comparing the algorithms using the four parameters, the one which shows superior performance will be used for the beamweight optimization.

1.4 Scope

An Important part to consider when evaluating the outcome of a thesis work is the scope. In this work, doppler estimation for single and multiple users is considered. Only the three propagation channels extended pedestrian (EPA), extended vehicular A (EVA), and extended typical urban (ETU) channels are considered. In addition, when considering multipath propagation in all the three channels, the doppler shift of each path is assumed to be the same. Eventhough, the system supports multiple users, there is no scheduling performed and every user will occupy the entire spectrum. Furthermore, separation of the different users signals at the receiver side and the effect of hardware impairments such as oscillator mismatch between the transmitter receiver are not considered.

1.5 Related Works

Doppler estimation in the uplink (UP) of an LTE system is a widely studied subject. In [2] frequency offset estimation in 3G LTE has been studied. The author proposes a frequency bins approach on the the DMRS symbols to estimate the frequency offset and compares the method with the cyclic prefix correlation in terms of the block error rate (BLER) and complexity. The estimation is done for a high speed train channel (HST) channel and considers no fading. In addition, it accumulates each user equipmemts (UE's) metric over a number of subframes before doing the estimation.

In [20] frequency offset estimation in Enhanced-Universal Terrestrial Radio Access (E-UTRA) is considered. Instead of comparing the demodulation reference signals (DMRS) and cyclic prefix methods, the author proposes a method which primarily uses the pilot method and combines it with the cyclic prefix method for an estimation range extension. The simulation mainly uses an HST channel for performance evaluation.

The autocorrelation function (ACF) of the DMRS symbols has been used in [22] to determine the speed and hence doppler frequency of a UE in an LTE uplink system. The method gives a biased estimation at lower doppler frequencies and hence requires a large number of subframes to compensate for that and for this reason it has not been considered in this thesis.

In [21], doppler frequency estimation based on the DMRS symbols is proposed. The method uses additive white gaussian noise (AWGN) and single tap Rician channels to demonstrate the performance.

As explained above, most of the research papers done on frequency offset estimation for an LTE UP consider the HST channel. Besides, a comprehensive comparison of the cyclic prefix and DMRS methods in the EPA, EVA, and ETU has not be done.

Most importantly, all of the publications focus on estimating the doppler but not using the estimation for reducing the complexity of an LTE beamforming system.

1.6   Report Organization

The paper begins by introducing the literature background which covers concepts of LTE, beamforming techniques, wireless channels and propagation models. In this chapter, doppler shift in wireless communications and specifically in orthogonal frequency division multiplexing (OFDM) systems will be covered. In chapter three, the various Doppler estimation techniques studied in the thesis will be presented together with the simulation set up and parameters used in the study. In chapter four, the results of the estimators with different fading channels will be given and analysis and comparisons of the results will be made and chapters five and six will cover the conclusion and future work respectively.

2

Theory

In this chapter the literature for the LTE system is briefly covered. The LTE multiple access schemes will be discussed and comparisons will be made.

2.1   LTE

The ever growing demand for high data rate communication has led to the development of LTE. It uses both TDD and FDD on the same platform. In the UP it implements single carrier frequency division multiple access (SC-FDMA) while in the DL it deploys orthogonal frequency division multiple access (OFDMA). The reason for implementing SC-FDMA in the UP is due to its low peak to average power ratio (PAPR) as will be discussed in detail later. LTE has an end user latency of less than 10 ms and a coverage range of 5-100km[8]. In addition, LTE allows the implementation of multiple input multiple output (MIMO) systems.

LTE supports bandwidths ranging from 1 MHz up to 20 MHz. This is due to the fact that the spectrum available varies for different bands and also for different operator conditions[8].

In both UL and DL, OFDM is used as the basic transmission scheme. In the time domain, the data is organized in terms of frames. Each frame has a duration of 10 ms. A single frame contains 10 sub-frames of each 1 ms duration. Each sub-frame contains 2 slots of 0.5 ms duration and 7 OFDM symbols[8]. A graphical desription of an LTE frame is shown in figure 2.1 below.
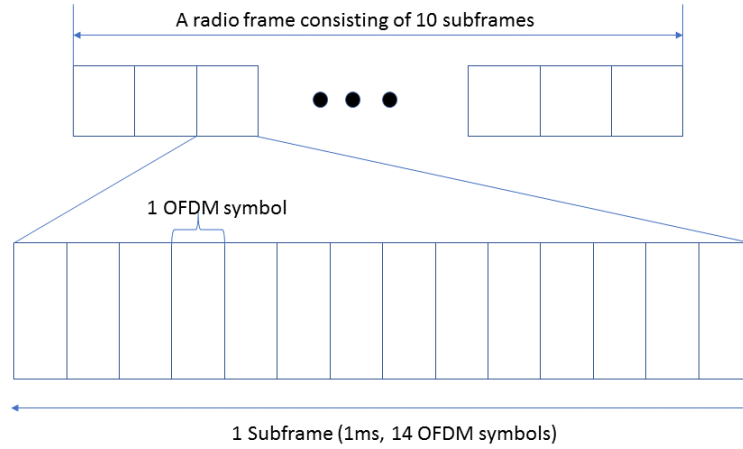
Figure 2.1: The LTE Frame Structure based on [18]

The subcarrier spacing of the OFDM system is 15 KHz. Therefore, the sampling rate of the system will be $15000 \times NFFT$. Where NFFT is the size of the fast fourier transform (FFT) [8]. The largest FFT size in the LTE system is 2048 giving a sampling rate of 30.72 MHz. This sampling rate corresponds to a bandwidth of more than 15 MHz. A detailed description of the LTE resources is given in table 2.1 below.

Bandwidth (MHz)	RB	NFFT	Subcarrier	Sampling rate (MHz)
1.4	6	128	72	1.92
3	15	256	180	3.84
5	25	512	300	7.68
10	50	1024	600	15.36
15	75	2048	900	30.72
20	100	2048	1200	30.72

Table 2.1: The LTE Resources

In LTE, three kinds of modulation schemes are used. Namely quadrature phase shift keying (QPSK), 16 quadrature amplitude modulation (QAM), and 64 QAM. As the order of modulation is higher, the data rate and spectral efficiency will increase. However, higher order modulation systems are more susceptible to noise and interference than the lower order schemes. Therefore, channel state information (CSI) should be used to choose between the different modulation schemes such that higher order modulations will be used if the channel is good and lower order schemes if the opposite is true.

2.1.1 LTE Physical Channels

In LTE, the physical channels are divided between the UL and DL.

2.1.1.1 Physical Down Link Channels

The physical DL channel consists of four main parts namely the physical downlink shared channel (PDSCH), physical broadcast channel (PBCH), physical control format indicator channel (PCFICH), and physical downlink control channel (PDCCH).

The PDSCH is used to transmit data and paging information in the DL [8].

The PBCH carries master information block (MIB), which is information transmitted by the Evolved Node B (eNB). The modulation type used is QPSK. The MIB is mapped on to 72 subcarriers or six resource blocks and it is transmitted every 40ms. One MIB contains 14 data bits, 10 spare bits and 16 cyclic redundancy check (CRC) bits [5].

The PCFICH gives the UE information about the received signal.It is transmitted on the first symbol of every subframe [5].

The PDCCH carries scheduling information regarding power control, resource allocation, and system information or paging. It contains DL control information which carries information for each UE [5].

2.1.1.2 Physical Uplink Channels

The Physical Uplink Control Channel (PUCCH) and Physical Uplink Shared Channel (PUSCH) constitute the physical uplink channel. The former carries information about scheduling, channel quality, and acknowledgements while the later is used to transmit data and paging information in the UL[8].

2.1.2 LTE Reference Signals

In LTE reference signals are used both in the UL and DL.

2.1.2.1 Uplink Reference Signals

There are two types of reference signals used in the LTE UL: DMRS and sounding reference signals (SRS). Figure 2.2 shows the location of the reference signals within a frame.
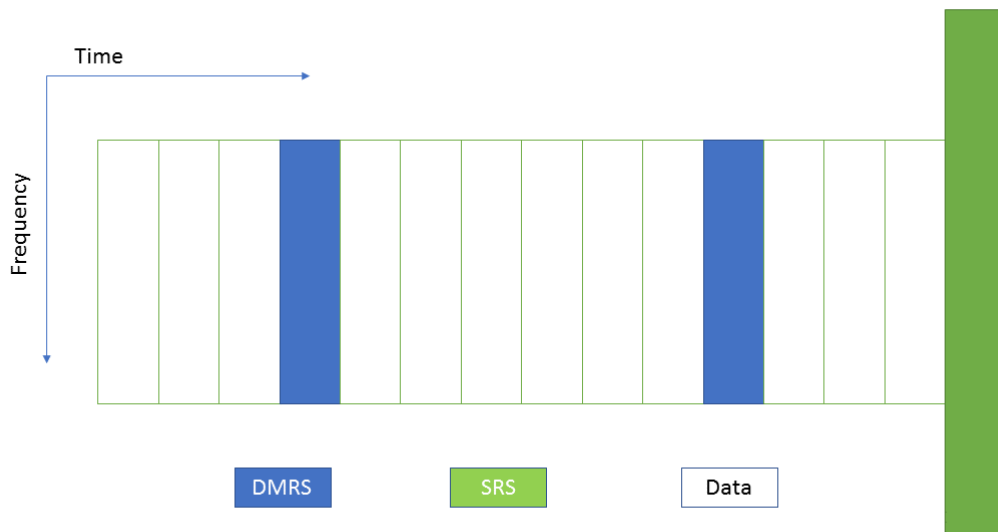
Figure 2.2: Uplink Physical Reference Signals

DMRS is transmitted together with the UL physical channels PUCCH or PUSCH and occupy the same bandwidth as the physical channels. It is used for channel estimation and coherent demodulation [8].

SRS is used by the base station for channel state information. This helps the receiver to know the channel quality over a wider bandwidth than the the bandwidth of interest. SRS is not necessarily transmitted in the same physical block with PUSCH as opposed to DMRS.

In LTE, there are three types of SRS transmissions namely single SRS transmission, periodic SRS transmission, and aperiodic SRS transmission.

In the single SRS transmission, as the name implies, the UE transmits the SRS only once. In periodic SRS transmission, the UE transmits the SRS in specific intervals ranging from 2-320ms. While in a aperiodic SRS transmission, the SRS is transmitted aperiodically based on triggering signals.

2.1.2.2   Downlink Reference Signals

In the DL, reference signals, which occupy specific positions in the physical structure, are transmitted for different purposes. Figure 2.3 shows the location of the reference signals with in a frame.
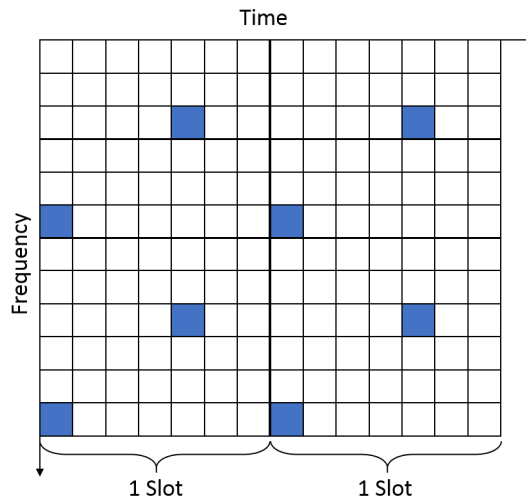
Figure 2.3: Downlink link Physical Reference Signals

The LTE DL system has several types of DL reference signals such as positioning reference signals, DMRS, CSI reference signals (CSI-RS), multicast-broadcast single-frequency network (MBSFN) reference signals, and cell specific reference signals (CRS) [8]. Each reference signal has a specific purpose.

Positioning reference signals are used for positioning the UEs. DMRS are used for channel estimation and coherent demodulation. CSI-RS are used for CSI in cases where the DMRS are not used for channel estimation. MBSFN reference signals are used for channel estimation for the multicast channel (MCH) cases. CRS are used for channel estimation and coherent demodulation [8].

2.1.3 Multiple Access Schemes in LTE

Two types of multiple access techniques are use in LTE: OFDMA and SC-FDMA. The first is used in the DL while the later is implemented in the UL. The use of OFDM has some advantages such as resistance to frequency selective fading, a base band receiver with low complexity, bandwidth flexibility and good spectral properties, compatibility with modern antenna technologies, and possibility of scheduling and also link adaptation [12].

OFDM system has also some drawbacks such as susceptibility for frequency offset and high peak to average power ratio (PAPR).

2.1.3.1 OFDMA

In OFDM modulation, the QAM modulated symbols are fed in to a serial to parallel converter. Then an IFFT operation is performed to change the frequency domain

symbols into time domain. OFDM converts a frequency selective wideband channel in to a number of narowband flat fading channels thereby reducing the effect of frequency selective fading. The IFFT of the QAM symbols is given in the equation below

$$x[n] = \frac{1}{\sqrt{N}} \sum_{i=0}^{N-1} X[i] e^{\frac{j2\pi in}{N}}, \tag{2.1}$$

Where x[n] is the time domain symbols, X[i] is the QAM modulated symbols and N is the total number of OFDM symbols.

After the IFFT modulation, cyclic prefixes are added to each OFDM symbols so that the effect of interference due to delay is effectively combated. Then the signal goes in to a parallel to serial converter to produce the baseband OFDM signal which is then up converted in to higher frequency by carrier modulation.

The transmitted signal will be corrupted by noise and fading so equalization and filtering is needed at the receiver side in order to recover the original signal [10]. The received signal is given by,

$$y[n] = x[n] * h[n] + v[n], \tag{2.2}$$

Where $y[n]$ is the received signal and $h[n]$ and $v[n]$ are the channel impulse response and additive noise respectively.

The receiver of an OFDM system is very similar to the transmitter but doing the exact opposite operation.

OFDMA is a multiple access technique where a group of OFDM modulated subcarries are allocated to different users. This allows for multiple users but with a reduced data rate.

In OFDMA, since the subcarriers are orthogonal to each other, the effect of frequency selective fading will be successfully counteracted. In addition, the subcarriers assigned to the different users will also be orthogonal thereby avoiding interference between the users. However, when the system experiences a frequency offset either due to an oscillator mismatch or doppler shift, the orthogonality between the subcarries will be destroyed and this leads to inter symbol interference (ISI) and multiple access interference (MAI).

Though, OFDMA has some interesting features as mentioned above, the presence of high PAPR makes it difficult for implementation in the UL of an LTE system. This is because, in the UL, the user terminals are the transmitters and power is of at most importance and a high PAPR leads to reduced amplifier performance and signal distortion.

The high PAPR in OFDMA is due to the application of IDFT on the QAM symbols. This makes the amplitudes of the transmitted symbols depend on the the constella-

tion points of the QAM symbols which leads to a high variation in the amplitudes of the transmitted symbols and hence in a high PAPR [11]

2.1.3.2 SC-FDMA

SC-FDMA is very similar to OFDMA. The main difference between the two is that, in OFDMA, the data symbols are directly mapped to the subcarriers, while in SC-FDMA, a discrete fourier transform (DFT) operation is performed on the data symbols before the subcarrier mapping. As a result, each subcarrier will contain a linear combination of all the transmitted data symbols there by making the system single carrier [11]. In the receiver side, an IDFT operation is preformed after sucarrier demapping.

SC-FDMA offers the same advantage as OFDMA in combating frequency selective fading. It also has a lower PAPR compared to the OFDMA and this makes the scheme very suitable for UL implementation. Therefore, low cost power amplifiers can be implemented in the UL.

2.1.3.3 Subcarrier Mapping in SC-FDMA

There are two types of subcarrier mappings in SC-FDMA: localized and distributed subcarrier mappings. In the first type of mapping, contiguous subcarriers are assigned to individual users while in the second scheme subcarriers distributed across the band will be assigned to users. Since the subcarriers are distributed across the frequency band, it provides frequency diversity. However, in channel dependent scheduling, the localized system will provide a higher data rate [11].

2.2   Beamforming Techniques

Beamforming is a technique used for directional signal transmission. When signals with the same frequency are transmitted in the same direction with the same polarization, some of them add up constructively and some cancel out each other. It is this property of signals that is used in beamforming to create spatial filters which can transmit signal in specific direction. Beamforming can be applied both at the transmitter and receiver and it is most commonly used in multiple input multiple output (MIMO) systems.

The MIMO technique increases the capacity in the high SNR regime by providing at most $N_{min} = \min(N_T, N_R)$ spatial degrees of freedom [4]. N_T and N_R are the number of transmitter and receiver antennas respectively. However, in most practical scenarios multiple users will be in communication with the base station giving rise to multi user MIMO (MU-MIMO) system which is depicted in the figure below.
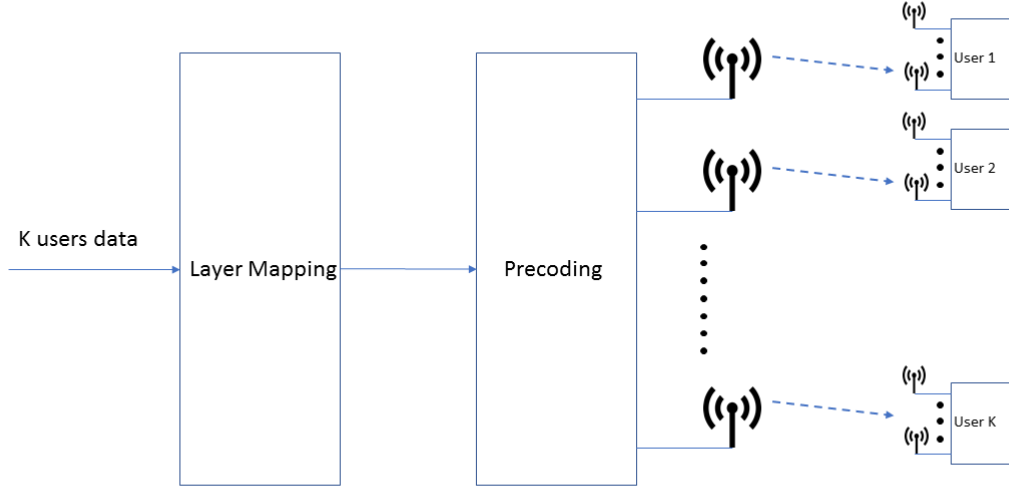
Figure 2.4: Downlink MU-MIMO based on [4]

For K users and N_T transmitter and N_R receiver antennas, the downlink configuration can be considered as a $(KN_T \times N_R)$ MIMO system [4].

$$y_k = H_k x + z_k, \tag{2.3}$$

$x \varepsilon C^{N_R \times 1}$ is the transmit signal from the basestation antennas. $y_k \varepsilon C^{N_T \times 1}$ is the received signal at the kth user, and $H_k \varepsilon C^{N_T \times N_R}$ is the channel between the base station and user k, and $z_k \varepsilon C^{N_T \times 1}$ is additive noise between the kth user and the base station antenna.

The signals from all users can be represented as

$$[y_1, y_2, ...y_K]^T = [H_1, H_2, ...H_K]^T X + [z_1, z_2, ..., z_K]^T, \tag{2.4}$$

The introduction of MU-MIMO has brought high performance improvement by combining MIMO with space division multiple access (SDMA)[19]. However, these systems suffer from the multi user interference (MUI) and interference between the antennas.

In order to combat the MUI in MU-MIMO, precoding techniques are used. The techniques can be both linear and non linear. The capacity achieving techniques are the non linear precoding techniques but their complexity is of a major disadvantage.

The linear precoding techniques, on the other hand, can achieve a reasonable performance with much lower complexity [19]. As a result, the linear precoding techniques are used in practical scenarios.

There are three types of linear precoding techniques. Namely, zero forcing (ZF), regularized zero forcing (RZF), and maximal ratio transmission (MRT).

2.2.1 Zero Forcing (ZF)

Zero forcing precoding is a method of combating the interference in an MU-MIMO system. It is simple to implement. However, it has a very high complexity as it involves inverting the channel matrix. The beamfroming weights are evaluated according to the equation below

$$W_{ZF} = H^H(HH^H)^{-1},$$ (2.5)

As can be seen in the equation, the ZF does not take the noise in to consideration in the weight computation. The regularized zero forcing (RZF) is an enhanced method of zero forcing precoding which considers noise and the unknown user interference in calculating the beam forming weights. The beamforming weights are calculated according to the following equation

$$W_{RZF} = H^H(HH^H + \alpha I_M)^{-1},$$ (2.6)

where α is given by

$$\alpha = \frac{K\rho^2}{p},$$ (2.7)

K is the number of UEs, ρ^2 is the noise power, and p is the downlink signal power.

2.2.2 Maximal Ratio Transmission (MRT)

Compared to the zero forcing and the regularized zero forcing algorithms, MRT has very low complexity. However, it suffers from multiuser interference.
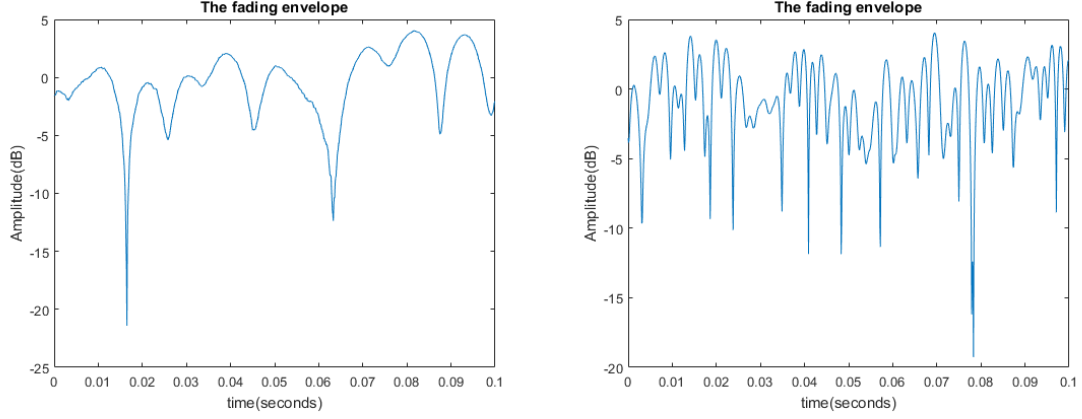
$$W_{MRT} = H^H,$$ (2.8)

2.3 Wireless Channels

In this chapter, the channel models used in the simulation environment are discussed and the effect of Doppler on the performance of the OFDM system is covered.

2.3.1 Fading in Wireless Channels

Fading is the random fluctuation of signal power. It can be classified as small scale and large scale fading.

(a) Signal envelope with a maximum Doppler of 55 hz

(b) Signal envelope with a maximum Doppler of 300 hz

Figure 2.5: Signal envelope for 0.1 seconds

2.3.2 Small Scale Fading

Fading that occurs due to signal propagation in multiple paths is called small scale fading. The fading occurs due to partial cancellation of the signal by itself.

Small scale fading can be further classified into fast fading, slow fading, flat fading and frequency selective fading. The classification is based on two important parameters called coherence time and coherence bandwidth. The coherence time of a fading channel is the time during which the characteristics of the channel are considered to be constant while coherence bandwidth is the bandwidth over which the channel exhibits constant characteristics.

Another important parameter of a fading channel is the delay spread which is defined as the time difference between the line of sight component and the latest multipath component. It is related to the coherence bandwidth by the following equation

$$B_c = \frac{1}{D},\qquad(2.9)$$

Where B_c and D are the coherence bandwidth and delay spread respectively. The coherence time of a wireless channel is given by

$$t_c \approx \frac{1}{f_d},\qquad(2.10)$$

14

where f_d and t_c are the maximum doppler frequency and the coherence time respectively.

When the coherence time of the channel is much larger than the symbol duration, multiple frequency components of the signal will experience the same or correlated fading. This type of fading is termed as slow fading. On the contrary, in fast fading, the coherence time of the channel is much smaller than the symbol duration. As a result, multiple frequency components of the signal will experience independent fading.

In flat fading, the coherence bandwidth of the signal is much larger than the signal bandwidth and the delay spread is less than the symbol period resulting in multiple frequency components of the signal experiencing the same or correlated fading. While in frequency selective fading, the coherence bandwidth of the signal is much smaller than the signal bandwidth and the delay spread is greater than the symbol period. As a result, multiple frequency components of the signal will experience independent fading.

In the simulation, three types of multipath propagation models are implemented namely Extended Pedestrian A model (EPA), Extended Vehicular A model (EVA), Extended Typical Urban model (ETU).

For EPA, the maximum doppler frequency and delay are 5 Hz and 410 ns respectively. Using equations 4.1 and 4.2, the coherence time and coherence badwitdhths become 0.2 seconds and 15.325 MHz respectively. Therefore, for a symbol duration of less than 0.2 seconds, the channel will be slow fading. Similarly for a signal bandwidth of less than 15.325 MHz, and symbol period of more than than 410 ns, the channel will be flat fading. For a frequency selective fading, the bandwidth of the signal and the delay spread are both greater than the coherence bandwidth and the symbol period respectively.

For EVA the maximum doppler frequency and delay spread are 70 Hz and 2510 ns giving a coherence time of 0.0143 seconds and a coherence bandwidth of 2.5 MHz. As a result, a symbol duration of less than 0.0143 will result in slow fading while a bandwidth of less than 2.5 MHz and symbol period of greater than the delay spread will give a flat fading profile. For a frequency selective fading, the bandwidth of the signal and the delay spread are both greater than the coherence bandwidth and the symbol period respectively.

For ETU the maximum doppler frequency and delay spread are 300 Hz and 5000 ns respectively. This results in slow fading for symbol period of less than 0.033 sec and flat fading for signal bandwidth less than 1.26 MHz and symbol period of greater than 5000 ns.

EPA	
Delay(ns)	[0 30 70 90 110 190 410]
Relative power(dB)	[0.0 -1.0 -2.0 -3.0 -8.0 -17.2 -20.8]
Max Doppler(Hz)	5
EVA	
Delay(ns)	[0 30 150 310 370 710 1090 1730 2510]
Relative power(dB)	[0.0 -1.5 -1.4 -3.6 -0.6 -9.1 -7.0 -12.0 -16.9]
Max Doppler(Hz)	70
ETU	
Delay(ns)	[0 50 120 200 230 500 1600 2300 5000]
Relative power(dB)	[-1.0 -1.0 -1.0 0.0 0.0 0.0 -3.0 -5.0 -7.0]
Max Doppler(Hz)	300

Table 2.2: Multipath channels used in the simulation

2.3.3 Large Scale Fading

Fading can also occur due to obstruction between the transmitter and receiver called shadow fading. Both path loss and shadowing are termed as large scale fading since the variation in power happens over large distances [10]. In the simulation model however, the effect of shadowing has not been considered.

A wireless signal experiences power degradation over distance. This is termed as path loss. The received signal at a distance d is given by:

$$Pr(dBm) = Pt(dBm) + 10\log(G) + 20\log(\lambda) - 20\log(4\pi) - 20\log(d), \quad (2.11)$$

where Pr(dBm) and Pt(dBm) are the received and transmitted powers in dBm, λ is the wave length and $\sqrt{G}$ is the product of the transmit and receive antenna field radiation patterns in the line of sight directions [10]

The path loss is the difference between the received and transmitted signal powers.

$$\text{Path loss} = Pr(dBm) - Pt(dBm) \quad (2.12)$$

The free space path gain is given by

$$\text{Path Gain} = -\text{Path loss} \quad (2.13)$$

2.3.4 Fading Models

Fading channels are described by statistical channel models. The two most commonly used methods are the Rayleigh and Rician fading channel models. The main

difference between the two is that in Rayleigh model, there is no line of sight between the eNB and UEs while in Rician fading there will always be a line of sight path.

Let the kth Rician or Rayleigh fading sample be $Z_k(t)$

$$
\begin{aligned}
Z_k(t) &= \sqrt{\frac{1}{1+K_k}} \sum_{n=1}^{N} \exp(j\omega_{d,k}t\cos(\frac{2\pi+\theta_{n,k}}{N}) + \phi_{n,k}) \\
&+ \sqrt{\frac{K_k}{1+K_k}} \exp[j(\omega_d t\cos(\theta_{o,k}+\phi_{o,k}))],
\end{aligned}
\tag{2.14}
$$

Where $\omega_{d,k}$ is the maximum Doppler frequency, K_k is the Rician factor, $\theta_{o,k}$ is the line of sight's angle of arrival. $\theta_{n,k}$, $\phi_{n,k}$, $\phi_{o,k}$ are mutually independent and uniformly distributed over $[-\pi, \pi)$ for all n and k. N is chosen between 8 and 12 for a good performance. For a Rayleigh fading channel, K_k,which it is the ratio of the line of sight component to the power scattered, is zero [3]

2.4 Doppler Shift In Wireless Communications

The relative movement between the transmitter and receiver causes variation in the received signal. Thus, signals arriving from different directions will experience a different frequency shift. This shift in frequency is known as doppler shift. The total phase shift experienced by an object moving with a speed of v is given by[16]

$$
\Delta\phi = \frac{2\pi v \Delta t}{\Lambda} cos\theta,
\tag{2.15}
$$

Where θ is the direction of arrival of the received signal relative to the direction of motion, Λ is the wavelength, v is the speed of the object, and $\Delta\phi$ is the total phase change. The wavelength is given by the equation below

$$
\Lambda = \frac{c}{f_c},
\tag{2.16}
$$

Where c is the speed of light and f_c is the carrier frequency. Using the above equation, the doppler shift is given by

$$
f_d = \frac{1}{2\pi}\frac{\Delta\phi}{\Delta t} cos\theta,
\tag{2.17}
$$

Equivalently the doppler shift can be given as

$$
f_d = \frac{v f_c cos\theta}{c},
\tag{2.18}
$$

From the above equation, the maximum Doppler shift occurs when θ is zero and it is given by

$$f_d = \frac{v f_c}{c}, \qquad (2.19)$$

2.4.1 Doppler spread

In a multipath propagation phenomenon, signals arrive at the receiver from multiple directions each with its own doppler frequency. The multipath is mainly due to reflections and scattering. When a single pulse is transmitted over a multipath channel, the received signal will be a pulse train with each pulse corresponding to the distinct multipath component. Therefore, the received signal has a larger bandwidth than the transmitted signal. This effect is known as doppler spread.
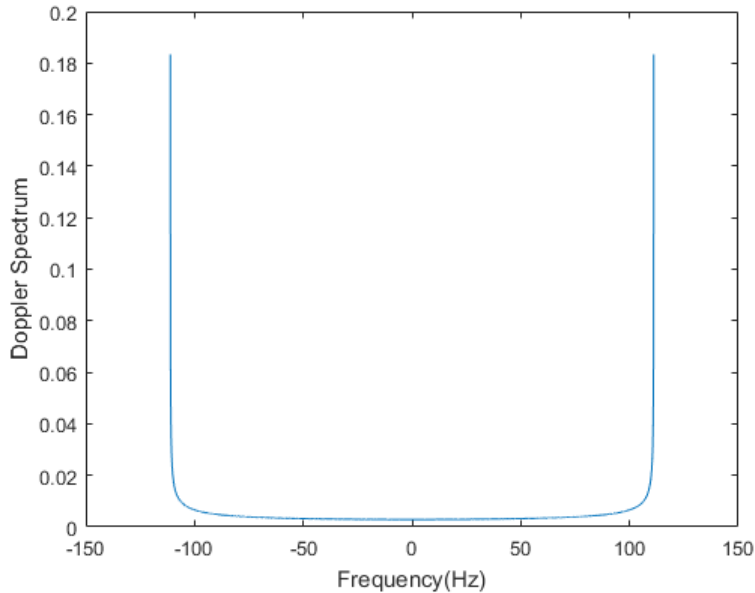
Figure 2.6: Doppler spectrum with $f_d = 110 Hz$

The maximum doppler frequency, f_d, will determine the amount of spread. For a carrier frequency of f_c the doppler spectrum will be in the range $[f_c - f_d, f_c + f_d]$.

2.4.2 Doppler Shift In OFDM

In an OFDM system, the kth received symbol is given by [15]

$$Y_k[n] = H_k[n]X_k[n] + Z_k[n], \qquad (2.20)$$

Where $X_k[n], Y_k[n], H_k[n]$, and $Z_k[n]$ are the nth frequency components of the kth transmitted symbol, received symbol, channel frequency response, and noise respectively.

18

The time domain received signal is given by

$$y_k[n] = IDFT\{Y_k[n]\} = \frac{1}{N}\sum_{n=0}^{N-1} X_k[n]H_k[n]e^{\frac{j2\pi(k+Nf_dT_s)}{N}}, \qquad (2.21)$$

Where Ts is the OFDM symbol time and f_d is the maximum Doppler frequency. As can be seen from equation 2.21, the relative movement between the UEs and eNB gives rise to a frequency offset equal to the doppler frequency. Therefore, knowing the maximum doppler frequency, it is possible to determine the speed.

In OFDM systems, the Doppler will cause performance degradation by increasing the the bit error rate of the system. This situation is depicted in the figure below.
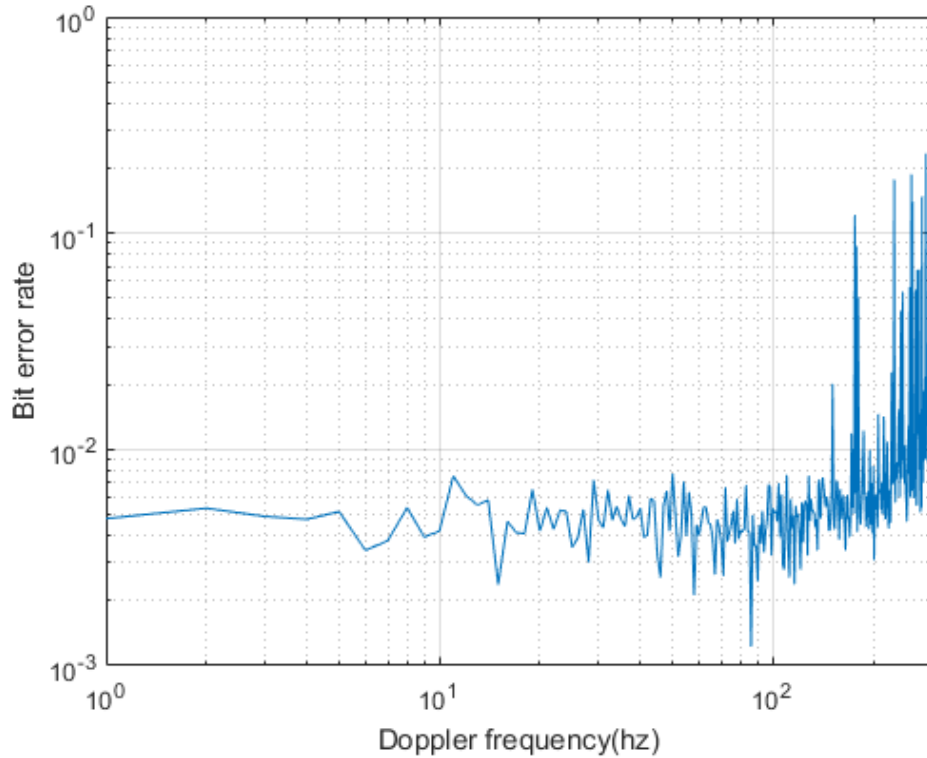
Figure 2.7: The effect of Doppler on bit error rate for an ETU channel with Rician Fading

3

Methods

3.1 Doppler Estimation

Since the doppler effect introduces a frequency offset, the estimation algorithms implemented in this thesis are based on frequency estimation. The two main methods of doppler estimation in the LTE TDD UP are the DMRS and the cyclic prefix methods.

The doppler is estimated by estimating the total phase difference between two repeated sequences in the signal.

$$f_d = -f_s \frac{\angle \gamma}{2\pi L}, \tag{3.1}$$

Where f_d is the doppler frequency, fs is the sampling frequency, γ is the correlation in time or frequency domain, and L is the correlation length.

The correlation in time domain is give by:

$$\gamma = \sum_{n=0}^{N-1}, r_n r_n^* \tag{3.2}$$

The correlation can also be done in frequency domain.

$$\gamma = \sum_{n=0}^{N-1} R_k R_k^*, \tag{3.3}$$

Where R_k and R_k^* are the FFT of r_n and r_n^* respectively which are two N length repeated sequences.

The two doppler estimation methods involve correlating the cyclic prefix and pilot symbols (DMRS).

3.2 Cyclic Prefix Correlation

The cyclic prefix correlation works by correlating the cyclic prefix of each received OFDM symbol with the complex conjugate of the corresponding OFDM symbol tail. If the time domain received signal is denoted by $r(n)$, then the FFT of the cyclic prefix and the OFDM symbols are given by [2]

$$R_{CP}(k) = \sum_{n=0}^{L_{CP}-1} r(n)e^{\frac{-j2\pi kn}{N_{FFT}}}, \tag{3.4}$$

$$R(k) = \sum_{n=0}^{N_{FFT}-1} r(n+N_{CP})e^{\frac{-j2\pi kN_{CP}}{N_{FFT}}}, \tag{3.5}$$

$$\gamma = \sum_{n=0}^{L_{CP}-1} R(k+k_o)R_{CP}^*(k+k_o)e^{\frac{-j2\pi kN_{CP}}{N_{FFT}}}, \tag{3.6}$$

Where N_{sc} is the number of sub carriers for an OFDM symbol, L_{CP} is the cyclic prefix length, and N_{FFT} is the FFT size, R and R_{CP} are the FFT of the received signal and the cyclic prefix respectively.

Once γ is determined, the Doppler freqeuncy can be calculated by using equation 3.1.

3.3 DMRS Symbol Correlation

The DMRS symbol correlation works by correlating the two DMRS symbols in a sub frame. As already discussed in the background, an LTE subframe contains 14 OFDM symbols of which the fourth and eleventh are DMRS symbols. If the received signal in a sub frame is denoted by a matrix x whose FFT is X, the correlation becomes

$$\gamma = \sum_{n=0}^{N_{sc}-1} X(n,4)X^*(n,11), \tag{3.7}$$

Once γ is determined, the doppler frequency can be found using equation 4.1. In addition, since the correlation is done for only two OFDM symbols, the method has a lower complexity compared to the cyclic prefix method.

Besides the two implemented algorithms in the project, three estimation methods have also been studied. Namely, the level crossing rate, the zero crossing of the auto correlation and the covarience methods.

3.4 Level Crossing Rate (LCR)

The level crossing rate of a signal is defined as the number of crossings per second of a signal for a given threshold level. The threshold value is usually set to half or $\frac{1}{\sqrt{2}}$ of the root mean square value [14]. The level crossing of a fading signal is given by

$$N_{LCR} = \sqrt{2\pi}\alpha e^{-\alpha^2} f_d, \tag{3.8}$$

Where α is the envelope threshold level to t he root mean square level, f_d is the doppler frequency, N_{LCR} is the number of crossings per second of the envelope for the given α. Solving for f_d gives

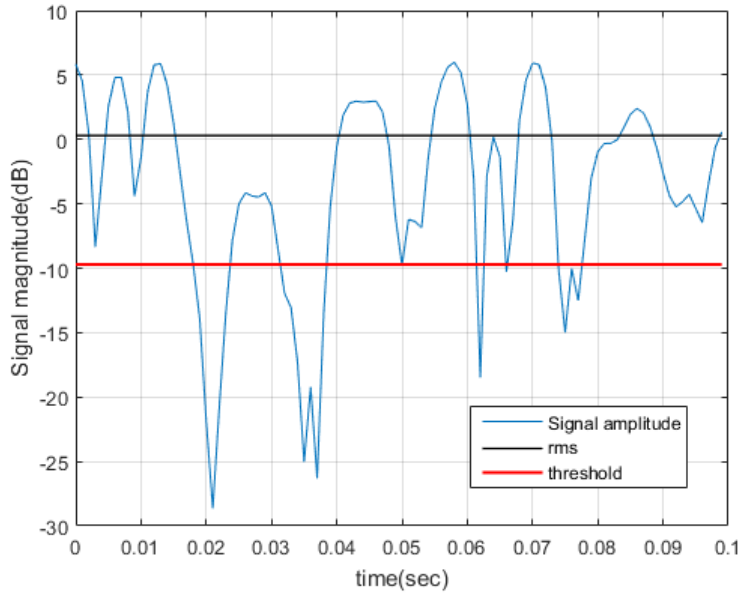$$f_d = \frac{N_{LCR}e^{\alpha^2}}{\sqrt{2\pi}\alpha}, \tag{3.9}$$

Figure 3.1: An example of level crossing rate of a signal

3.5 Doppler Estimation Based On Zero Crossing of Autocorrelation Function

The zero crossing of the auto correlation [13][1] uses the correlation proprieties of the fading channel in that the auto correlation of the channel impulse response resembles

the Bessel function of the zeroth order. If the channel impulse response is given by $h(t)$, then its auto correlation will resemble the zeroth order Bessel function.

$$r_{hh}[n] = J_o(2\pi f_d T_s k),\tag{3.10}$$

Where r_{hh} is the correlation of the channel impulse response and J_o is the Bessel function of the zeroth order. Therefore, by finding the lag value for which the auto correlation of the channel response is zero, one can determine the doppler frequency.

The doppler is estimated using the following formula.

$$f_d = \frac{2.4048}{2\pi k T_s},\tag{3.11}$$

Where k is the lag value for which the auto correlation is zero and T_s is the sampling time. The lag value is usually determined by using the interpolation method. In general, the zero crossing method can be summarized as follows:

1. Find the autocorrelation function of the channel impulse response

2. Using the in-phase component of the calculated autocorrelation function, find the first smallest positive value and the first maximum negative value

3. Find the zero crossing point using the two selected points by applying interpolation

4. Calculate the doppler frequency using equation 4.10

However, as can be seen from equation 4.10, a smaller doppler value corresponds to a very high lag value which in turn requires large number of samples. In order to solve this challenge [1] divides the doppler estimation in to slow and fast modes before performing the estimation. In addition, using the inverse Bessel function at the receiver can increase the complexity of the receiver. For this reason, a look up table is usually used.

3.6 Doppler Estimation Based On Sample Correlation

This method which is proposed in [17] uses the spectral moments of the received signal to find the doppler frequency. The method estimates the maximum doppler frequency by using the equation below

$$f_d = \sqrt{\frac{-r_{hh}''(0)}{r_{hh}(0)}},\tag{3.12}$$

In this method, the result of the channel impulse response correlation, with a specified number of lags, will be approximated by a second order polynomial using the Taylor series approximation. This will solve the problem of finding the root for a higher order polynomial [17]. The steps followed in this method can be summarized as follows:

1. Find the correlation estimates $\{\hat{r_{hh}}(lT_s)\}$ by using sample averaging

2. Calculate $\hat{a_k}=\mathrm{argmin}_{a_k}\sum_{l=0}^{L} |\hat{r_{hh}}(lT_s)\} - \sum_{k=0}^{2} a_k l^k|^2$

3. Calculate $\hat{r_{hh}}^{(n)}(0) = \frac{n!\hat{a_n}}{T_s^n}$ $n=0,2$

4. Use the result from step 3 into equation 4.12

In the above steps, L is the number of lags in the correlation. However, since these algorithms require a large number of samples, they were not implemented due to the limitation of the simulation environment. Their complexity is analyzed and compared with the two implemented algorithms.

3.7   Complexity Analysis

The cyclic prefix correlation works on a sub frame basis. Each UL sub frame has 14 OFDM symbols. The cyclic prefix of each OFDM symbol will be correlated with corresponding tail and the result is added. Therefore the complexity in terms of the number of complex multiplications for a sub frame will be:

$$C = ML_{CP}, \tag{3.13}$$

Where M is the total number of OFDM symbols and L_{CP} is the length of the cyclic prefix.

The complexity for the DMRS correlation can be calculated in the same manner. Since the method involves correlating the two pilot symbols in a sub frame, it has a lower complexity compared to the cyclic prefix method. The complexity in terms of the number of complex multiplications is given by:

$$C = N_{sc}, \tag{3.14}$$

In order to calculate the complexity of the auto correlation and the covarience method, it is important to start from the definition of auto correlation. The auto correlation of a sequence given by $r[n]$ is defined as

$$r_{xx}[l] = \sum_{l=0}^{L-1} r^*[n]r[n - l] \tag{3.15}$$

Where L is the total number of lags. From the formula, it is easy to see that for each lag value l, there are $N - l$ complex multiplications. Where N is the total number of

samples of the received signal or the channel impulse response. Therefore, the total complex multiplications becomes:

$$
\begin{aligned}
C &= \sum_{l=0}^{L-1}(N-l) \\
&= \sum_{l=0}^{L-1} N - \sum_{l=0}^{L-1} l \\
&= NL - \frac{L(L-1)}{2} \\
&= NL - \frac{L^2 - L}{2} \\
&= \frac{L(2N+1-L)}{2},
\end{aligned}
\tag{3.16}
$$

The Taylor series approximation involves inverting a matrix of size $(L \times L)$. Which leads to L^2 complex multiplications. Therefore, the number of complex multiplications in the covarience method is given by

$$
C = L^2 + \frac{L(2N+1-L)}{2},
\tag{3.17}
$$

The zero crossing of the auto correlation involves a correlation of the channel impulse response of length N. The result of the operation is then followed by a search from the peak until the first minimum (negative) value is located. Then, interpolation to find the doppler. The length of this search depends on the doppler. The smaller the Doppler, the larger the search length and vice versa. Compared to the auto correlation, the searching and interpolation have negligible complexity. Therefore, the total number of complex multiplications can be found directly from equation 3.17.

As mentioned earlier, the level crossing method works by counting the total number of times, the signal envelope crosses a certain threshold. Calculating the threshold of the signal involves finding the root mean square of the signal. This implies, for a signal of length N, the total number of complex multiplications becomes N. Complexity comparison of the different algorithms is shown in the figure below.
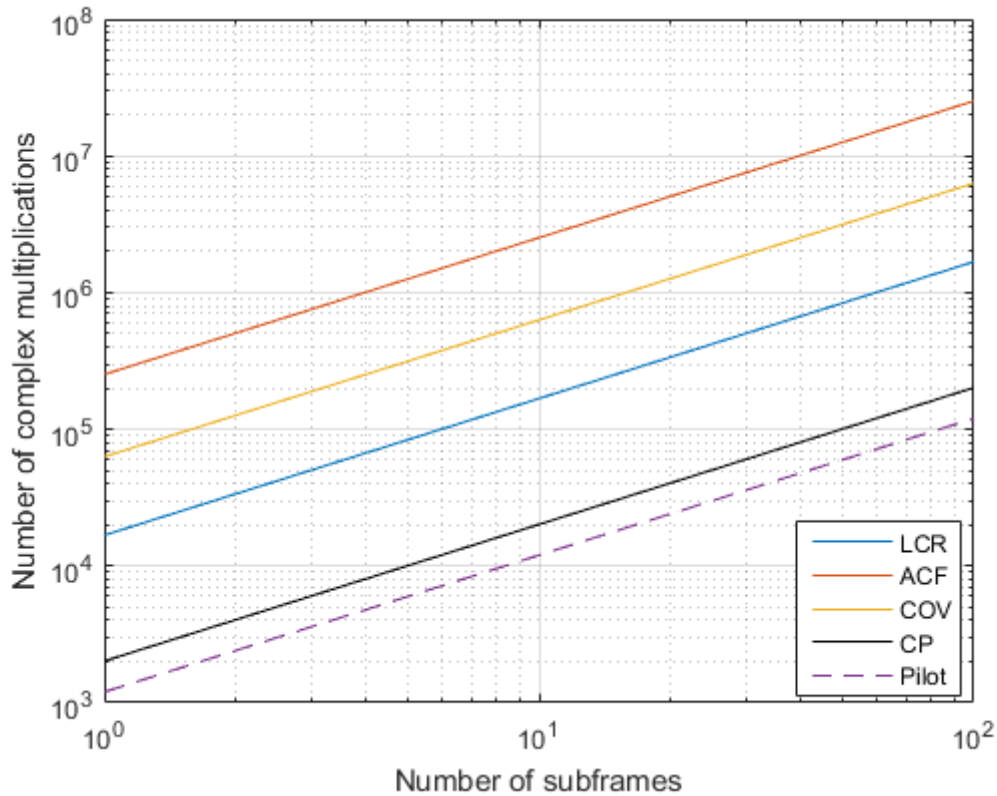
Figure 3.2: Complexity Comparison of Doppler Estimation Algorithms

3.8 Simulation Setup

3.9 Matlab Model

The Matlab model used is constructed so that testing and comparison with different parameters is easier. It is possible to set channel and link parameter using the set up. Besides, it includes support for the displaying the results of the simulation in terms of bit error rate (BER) and constellation diagrams.

To have an overall understanding of the model, the following list summarizes all the functionalities that the model supports

- Four Delay profiles EPA, EVA, ETU, and a custom channel

- TDD transmission in both the uplink and downlink

- Three modulation schemes QPSK, 16QAM, 64QAM

- The number of antennas and UEs can be changed

- Five LTE bandwidths 1.4-20 MHz

- ZR, RZF, and MRT beamformings

- Perfomance display in terms of bit error rate and constellation diagrams

3.10 Channel and Link Setups and Transmission

The channel setup process involves setting several parameters. In this process the number of eNB and UE antennas, the number of layers of transmission, transmission bandwidth, carrier frequency and delay profiles are set.

The user can also add multiple UEs. The number of UE antennas must also be at least equal to the number of layers of transmission. The choice of the system bandwidth affects the number of subcarriers used in the simulation as it is described in the theory part. The delay profile has four options EPA, EVA, ETU, and a custom made channel model. It is important to note also that the length of the channel in time is equal to the number of subframes so that the frames are time correlated and continuous. Another key point to point out here is that, since the channel generation stage is one of the time consuming parts of the simulation especially when the number of basestation antennas and subcarriers are high, it is resued multiple times with diffrent link set ups.

In the link setup, the modulation scheme is chosen. As described above, three modulation methods are available: QPSK, 16QAM, and 64QAM. In the link, one subframe is sent in the UL and the channel is estimated which is then used for calculating the beamforming weights using any of the available methods. The DL frame, which is weighted with the weights, will then be sent to the UE.

3.11 Uplink

In the UL, the data from each UE is transmitted in the PUSCH to the eNB. The DMRS symbols located in each PUSCH data symbols will be used to estimate the

channel. The least squares channel estimation method is used to estimate the channel between the UE and eNB. The whole bandwidth is estimated in the estimation so that the beamforming algorithms get sufficient information.

The received grid will also be equalized using the result of the channel estimation. For this purpose, a simple frequency domain equalization is implemented.

3.12   Downlink

At the eNB, all the users grids are created using the steps shown in figure 1. Each UE will be assigned the entire grid. Each of the grid will be weighted using one of the beamforming algorithms before transmission. The signal received at the UE will pass through the receiver process shown in figure 1.

3.13   Simulation Parameters

Four delay profiles namely EPA, EVA, ETU, and one custom channel, with the delay profile shown below, have been used in the simulation. The main reason to use the custom channel is due to the fixed value of the maximum doppler frequency in all the remaining channels and it was necessary to go to higher frequencies especially when comparing the two algorithms in terms of estimation range. Even though, there were three modulation techniques in the matlab set up, only the QPSK method has been used in the simulation process. Besides, out of the five available bandwidths in the LTE set up, only the 20MHz bandwidth is used for analysis. In order to compare the performance of the two algorithms, the doppler of each path is kept at the maximum value.

Path Delay = [0 30 70 90 110 190]$\times 10^{-9}$;

Average Gain =[0 -1 -2 -3 -8 -17.2];

Note that, in the simulation results, the true doppler value corresponding to the three channels EPA, EVA, and ETU are 5, 70, and 300 Hz respectively. Table 3.1 summarizes the simulation parameters used in the study.

Modulation	QPSK
BW (MHz)	20
Duplex	TDD
Sampling Frequency(MHz)	30.72
FFT	2048
Carrier Frequency(MHz)	5000
Number of Transmitter Antennas	1
Number of Receiver Antennas	8
Frame Size	10 millisecond
Sub frame size	1 millisecond

Table 3.1: Simulation parameters

4

Results

The doppler estimation has been done for both Rayleigh and Rician fading channels. In this chapter the simulation results for the DMRS and the cyclic prefix methods will be compared and analysis will be given. Their performance is measured in terms the mean of estimation for a range of SNR values, the normalized mean square error (NMSE), and estimation range.

As stated in the planning stage of the thesis, the implemented algorithms will be compared in terms of the four parameters: performance with SNR, estimation range, NMSE, and complexity. As the complexity has been covered in the previous chapter, emphasis will be given to the three remaining parameters.

4.1   NMSE

To compare the NMSE of the two methods, the number of iterations in the simulation is set to 100. The main reason for choosing this value is to limit the simulation time. The NMSE of the two estimators has been compared for Rayleigh, Rician, and the custom made channels. The measurement is done by varying the SNR from -5 dB - 20 dB and recording the total BER.

From figures 4.1-4.3, it is clearly shown that the DMRS method has a smaller NMSE. The performance of the methods improve with SNR. For the DMRS method, a significant improvement with SNR is seen in the EPA channel. However, for custom channel, the improvement with SNR tend to saturate after an SNR of 5 dB. One important thing to notice here is that, both methods has shown performance improvement in the custom channel compared to the EPA case. This is due to the fact that the custom channel has a smaller path delay compared to the EPA case. On the other hand, for the cyclic prefix method, considerable performance improvement can be observed from negative SNR values towards 0 dB. However, the difference in performance, in terms of accuracy, after 0 dB is very small.
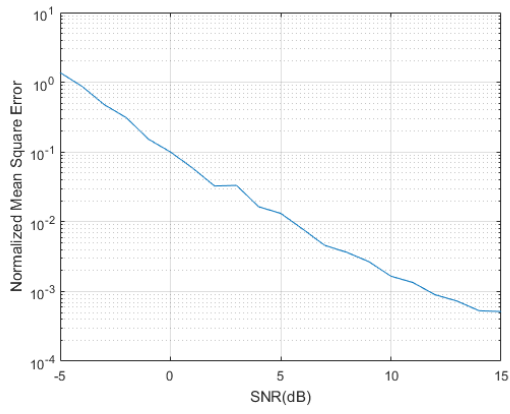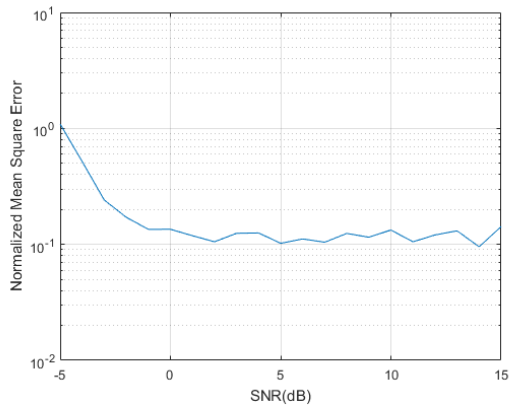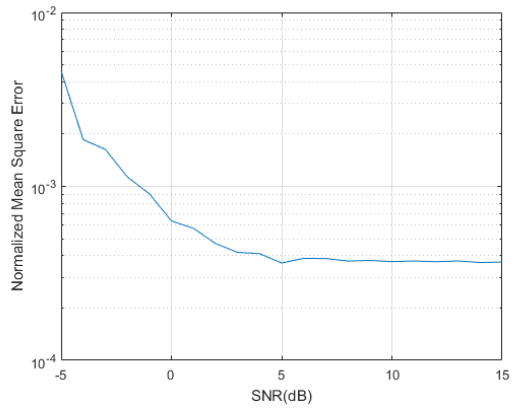
(a) DMRS
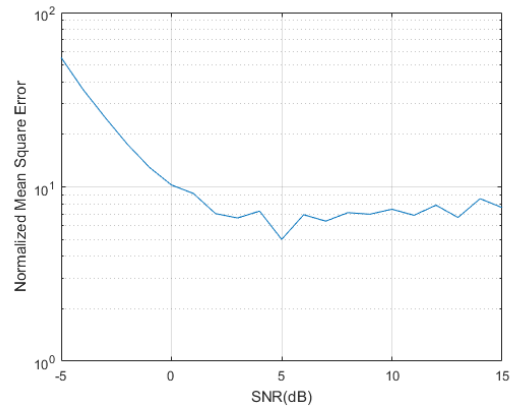
(b) Cyclic prefix

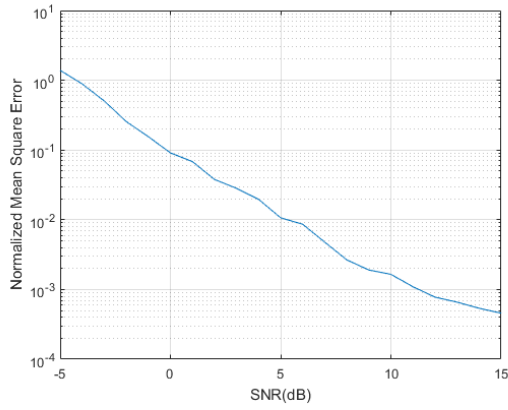**Figure 4.1:** NMSE for EPA with Rayleigh fading
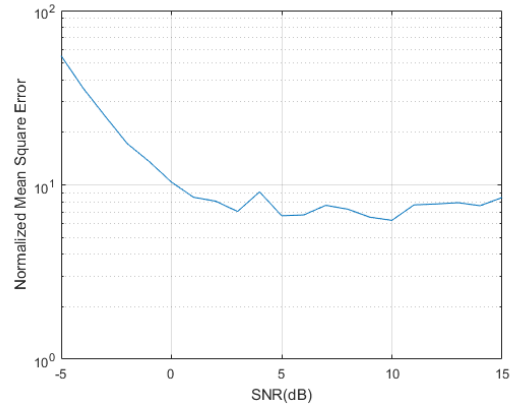

(a) Cyclic prefix

(b) DMRS

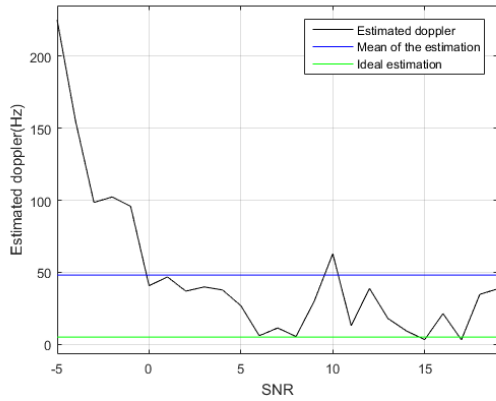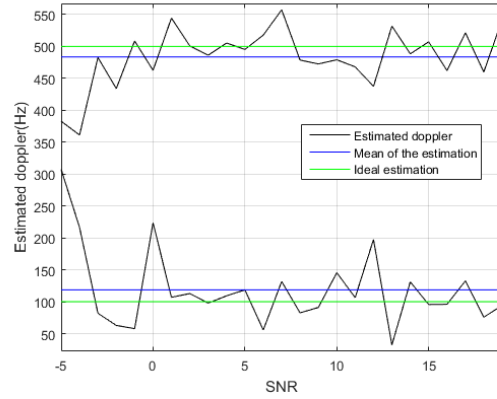**Figure 4.2:** NMSE for Rayleigh fading with custom channel

(a) DMRS

(b) Cyclic prefix

Figure 4.3: NMSE for EPA with Rician fading

(a) Cyclic prefix for EPA

(b) Cyclic prefix method for the custom channel with true doppler of 100 and 500 Hz

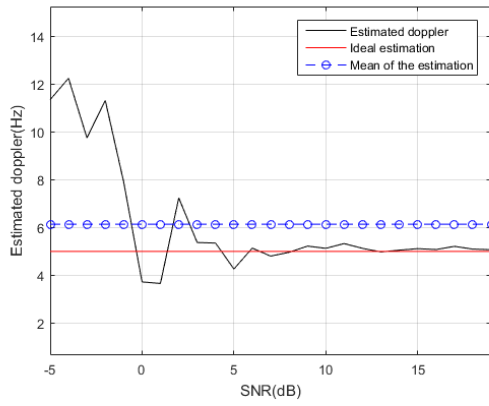**Figure 4.4:** Performance with SNR for the cyclic prefix method for Rician fading

4.2 Performance With SNR

The comparison made in the NMSE part mainly focuses on the EPA and custom channels. For this reason, in this part the result of the estimators over different channel types will be discussed. In order to display the performance of the algorithms with SNR, the estimation results of the methods over a range of SNR values are displayed. In addition, to give an indication of the overall performance, an average of the estimation over the entire SNR range is calculated.

Figures 4.4-4.7, show the performance of the estimators with SNR. In figure 4.4, the cyclic prefix estimation for the EPA and custom channels is displayed. In the EPA case, the average of the estimation shows a large deviation from the true value.

On the contrary, for the custom channel, the average value of the estimation is closer to the true value showing significant improvement compared to the EPA case. An important thing to observe here is that, in the case of the EPA channel, the maximum doppler frequency is 5 Hz while for the custom channel, the maximum doppler was set to 100 and 500 Hz. From this observation, we can see that the cyclic prefix method gives a biased estimation at lower doppler frequencies. This effect is also observed in the custom channel in that the average of the estimation in case of 500 Hz is more closer to the true value compared to the one in the 100 Hz case. The same scenario is covered in figure 4.7. In another case, figure 4.5 shows the performance of the DMRS method in four channel conditions. A more accurate estimation has been observed in case of EPA and the custom channels. This is expected given the less dispersive nature of the channels. However, for the ETU channel, the average of the estimator is a little bit larger than the true doppler due to the high dispersive nature of the channel. The same observation can be made in figure 4.6.

From the results observed, in figures 4.4-4.7. It is possible to conclude that the DMRS method shows a better estimation accuracy. Besides, the performance of the estimators is dependent on the SNR. This is clearly depicted in the figures. The result of the estimators is well off the ideal value in low SNR conditions. However, for higher SNR values, the average estimation is closer to the ideal value.
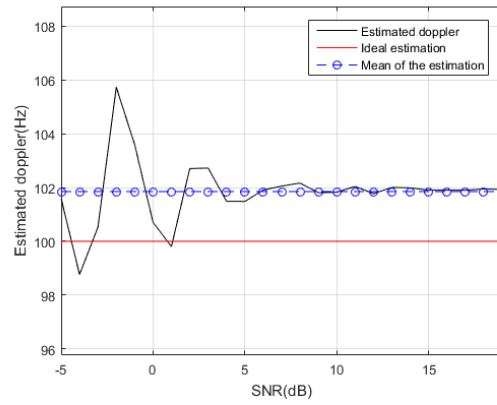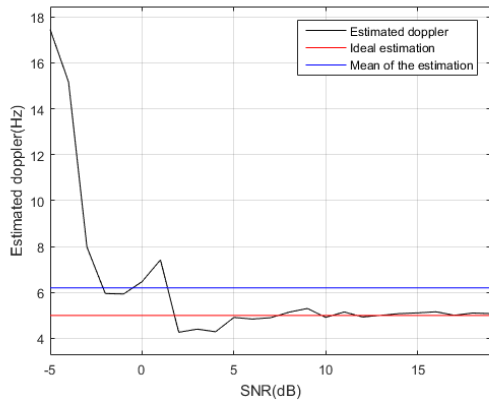
(a) DMRS for EPA
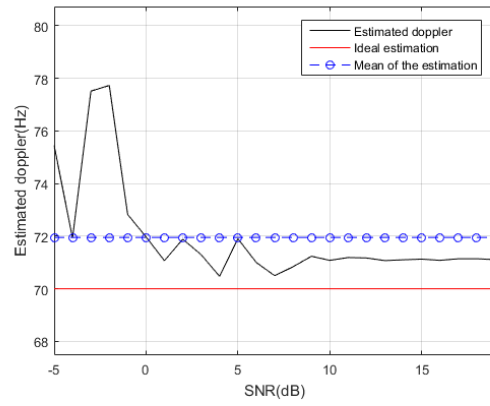
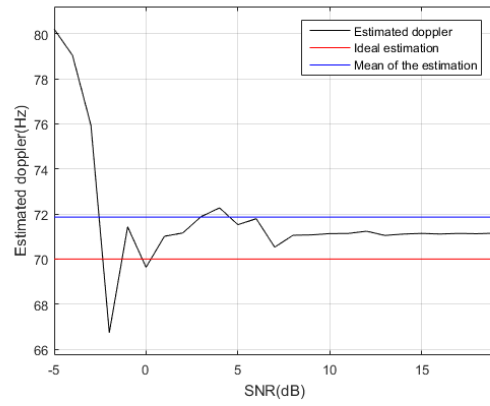(b) DMRS for EVA
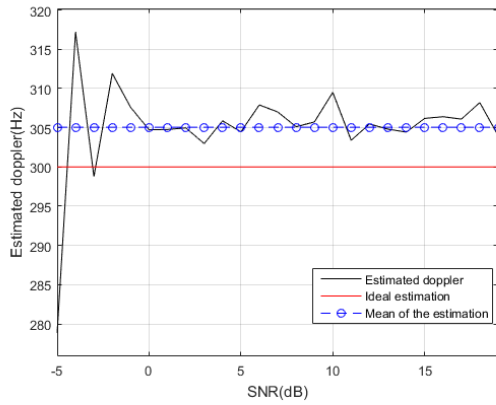
(c) DMRS for ETU

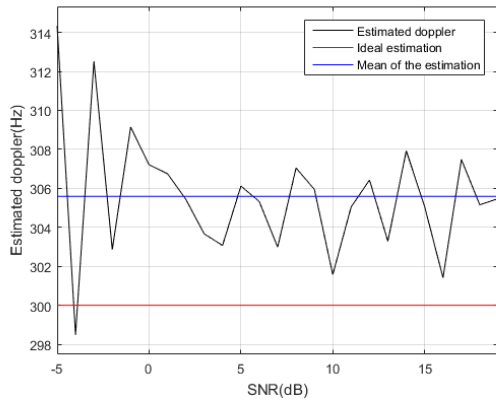(d) DMRS Method for the custom channel with true doppler of 100 Hz

Figure 4.5: Performance with SNR for the DMRS method with Rayleigh fading
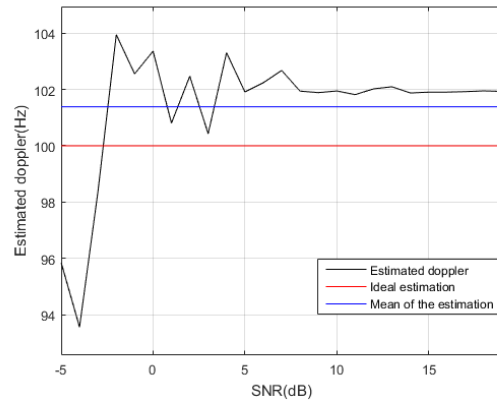
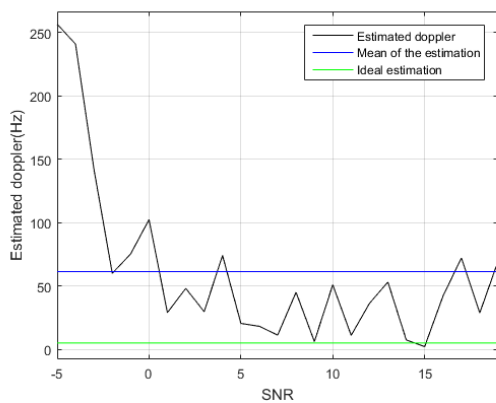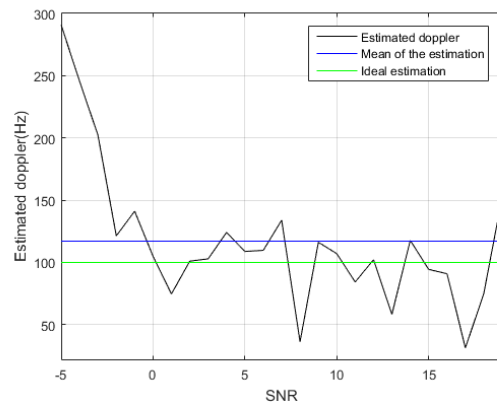(a) DMRS for EPA

(b) DMRS for EVA

(c) DMRS for ETU

(d) DMRS for the custom channel with true Doppler of 100 Hz

Figure 4.6: Performance with SNR for the DMRS method with in Rician fading
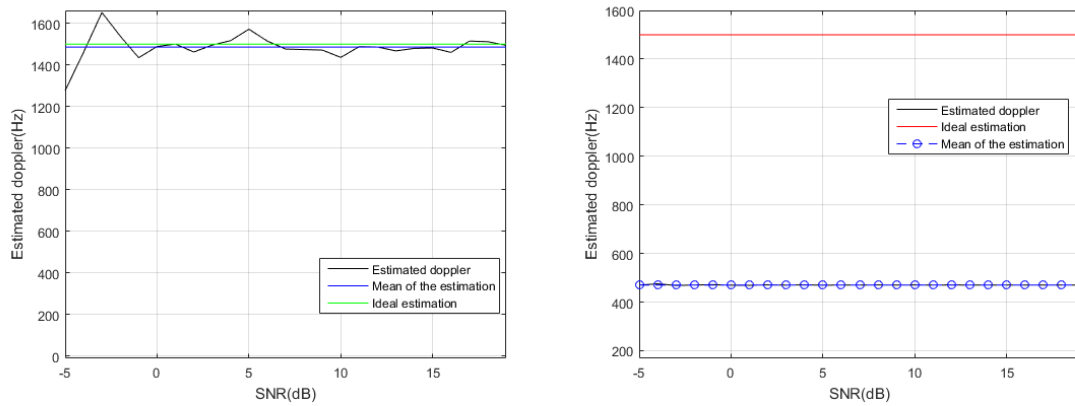

(a) Cyclic prefix for EPA

(b) Cyclic prefix for flat fading with true doppler of 100 Hz

Figure 4.7: Performance with SNR for the cyclic prefix method for Rayleigh fading

4.3 Estimation Range

Since the separation between the two DMRS symbols in a sub frame is 0.5 millisecond, the maximum frequency offset which can be estimated, according to Nyquist criterion, is 1000 Hz. On the contrary, for the cyclic prefix method, a frequency offset of up to half the sub carrier spacing, $(-7500, 7500)$ Hz, can be estimated. The result shown in figure 4.8 clearly shows this case. As can be seen in the plot, the cyclic prefix method is able to estimate a doppler of 1500 Hz with the mean of the estimation quite close to the ideal value. However, for the DMRS method, there is a considerable gap between the mean of the estimator and the true value making the scheme impractical for doppler values exceeding 1000 Hz.


(a) Cyclic prefix   (b) DMRS

Figure 4.8: Comparison of the two estimators in Rayleigh fading custom channel with a maximum doppler of 1500Hz

4.4 Multi User Single Input Multiple Output (MU-SIMO)

The DMRS method has also been appl ied for multiple users where each user has a single transmitter antenna communicating with four eNB antennas. Each user is assumed to have the same doppler. As can be seen in figure 4.9, the method works well in all channel cases. Compared to ETU, an improved performance is seen for the custom channel, EPA, and EVA. In fact for EPA the result of the estimation is almost the same as the true value for each user. This is because the signal experiences a relatively samll variation over several OFDM symbols. However, for the ETU channel, the estimation deviates from the true value due to the high dispersive nature of the channel.
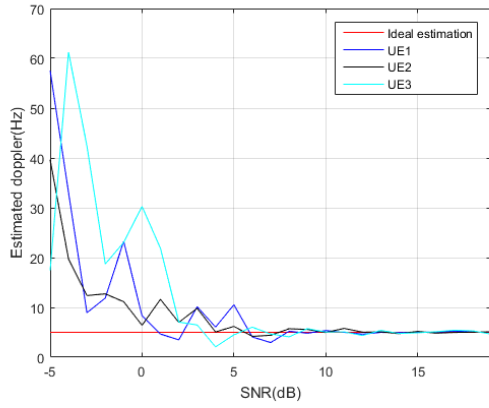
(a) DMRS for EPA
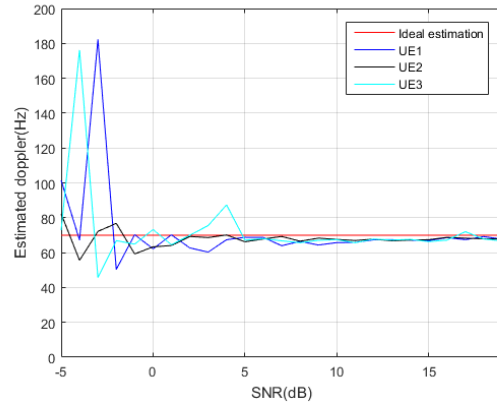
(b) DMRS for EVA
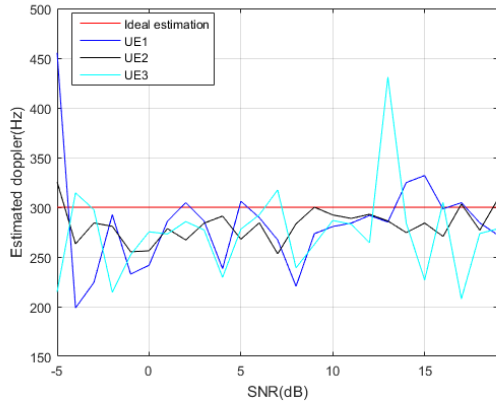
(c) DMRS for ETU
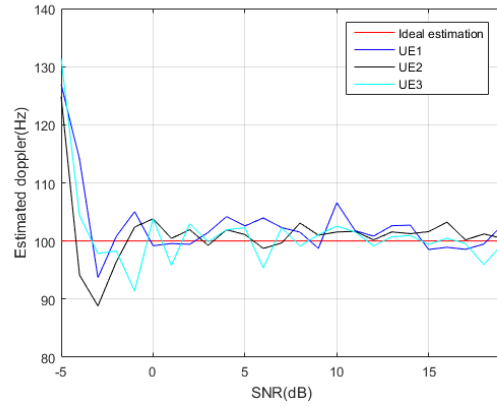
(d) DMRS forthe custom channel with true doppler of 100 Hz

Figure 4.9: Performance with SNR for the DMRS method in Rayleigh fading

4.5 Using The Doppler Estimation For Reducing The Beam Weight Computation

The beam forming system involves an enormous amount of complexity. Considering the system under study, the main sources of complexity are the channel estimation and the precoding stages. This can be seen from equation 2.5. For a channel matrix, H, of size $(N \times M)$, where N is the number of subcarriers and M is the total number of OFDM symbols in a subframe, the complexity is of $O(N^3)$. In the case of a 20 MHz bandwidth, the number of subcarriers per user can reach up to 1200 which leads to a considerable amount of complexity.
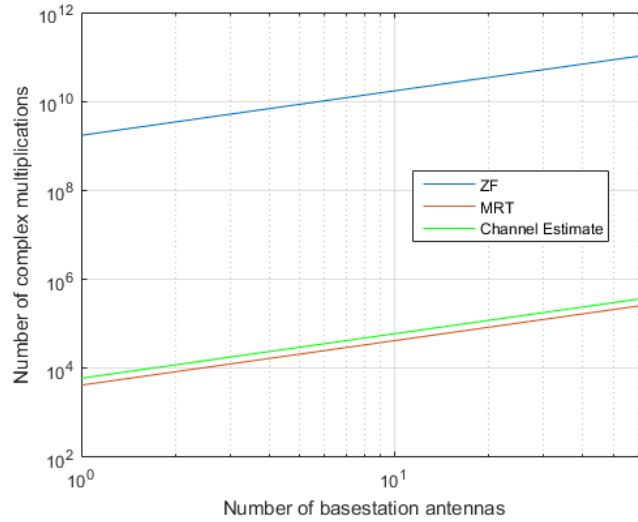
Figure 4.10: Complexity of the channel estimation and precoding

Figure 4.10 shows the complexity of the channel estimate and the beamforming techniques. As can be seen in the figure, the complexity of the the ZF is considerably large especially with the increase in the number of eNB antennas. On the contrary, the MRT technique has a much lower complexity compared to ZF but at the cost of reduced performance.

The doppler estimation is used to reduce the complexity by providing an estimate of the coherence time. Once the coherence time is estimated from the doppler, the total number of sub frames for which the duration is less than or equal to the coherence time is found. Using this frame number, the precoding and channel estimation stages were skipped after they are performed once. In order to have a clear performance control, an arbitrarily chosen DL BER of 10^{-12} is used and a sequence of DL subframes were sent until the BER exceeds this value.

The test was done for the three channels: EPA, EVA, and ETU and considers the three beamforming techniques. As shown in figure 4.11, the highest performance gain has been observed for EPA. This is expected as the signal experiences a small variation over large number of frames. For this channel, more than 100 DL sub frames can be sent with the same beam forming weight. This implies that the channel estimation and the beam weight computation can be reused for at least 100 subframes. For EVA, the number of DL subframes that can be sent with the same beamforming weights is smaller. This is expected as the signal experiences quick variation over small number of frames. For this channel, on average, $5 - 7$ DL subframes can be sent with the same beamforming weights.
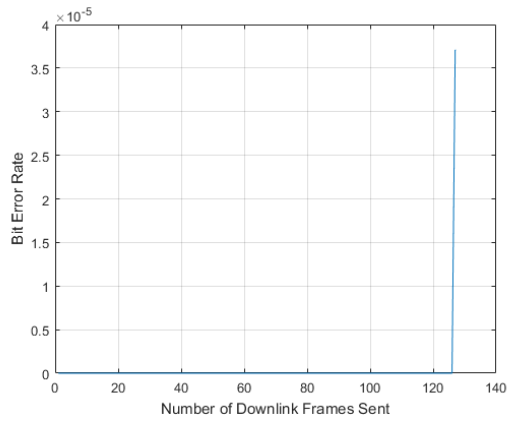
(a) EPA
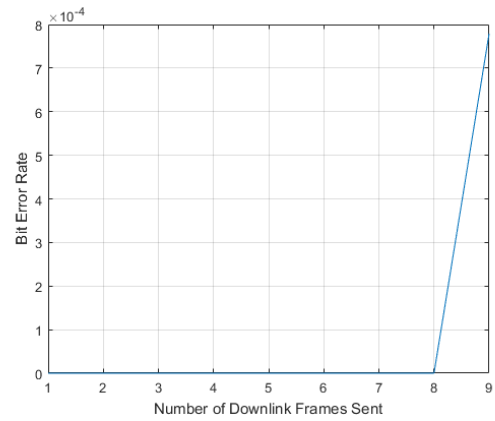
(b) EVA

Figure 4.11: Applying the doppler estimation for the beam weight optimization

The results depicted in figure 4.11 are one time cases. However, the experiment had been done a number of times and tables 4.1 and 4.2 show the number of DL subframes sent with the same weights in five test cases for EPA and EVA respectively. Since the ETU channel is a highly dispersive channel, beam weight optimization can not be applied.

Test	Number of DL subframes sent with the same weight
1	106
2	112
3	124
4	130
5	108

Table 4.1: Test for optimization in EPA at an average UL SNR of 8 dB and DL SNR of 20 dB

Test	Number of DL subframes sent with the same weight
1	7
2	9
3	8
4	8
5	6

Table 4.2: Test for optimization in EVA at an average UL SNR of 8 dB and DL SNR of 20 dB

5
Conclusion

In this thesis work, two methods of doppler estimation in the LTE TDD UL namely the DMRS and the cyclic prefix methods have been studied. As stated in the planning stage of the thesis, the methods have been compared in terms of the NMSE, complexity, performance under noise, and estimation range. From the results obtained in chapter 4, it can be concluded that the only criteria where the cyclic prefix method beats the DMRS method is in the estimation range. In all the remaining cases the DMRS method shows superior performance.

The estimation of the doppler has also been used to optimize the performance of the beamforming system by reducing the complexity involved in the beamweight computation and channel estimation. It has been shown that for less dispersive channels such as EPA, the complexity can be reduced to a great extent. However, for highly dispersive channels such as ETU, the estimation can not be used to reduce the complexity.

6

Future Work

This thesis work focuses on estimating the doppler and using the the result of the estimation for optimizing the beamweight computation. When multiple users share a spectrum, the carrier frequency offset due to doppler and hardware impairments will degrade the performance of the system by causing interference. One interesting area is to explore for low complexity algorithms which can successfully separate the different users signals while suppressing the interference at the same time. In fact, this has been a very active research area and many papers which focus on interference suppression have been published over the past decade [9]. Furthermore, as discussed in the results part, the optimization is done for a single user occupying the entire spectrum and assuming that each component of the multipath is having the same doppler. Therefore, as a future work, one can study complexity reduction for multiple users sharing a spectrum and with each component of the multipath having a different doppler. In addition, the results of the optimization are done for a single case where the UL and DL SNR values are fixed. For this reason, testing the optimization for a range of SNR values could also be considered as a future work. Extending the range of estimation of the DMRS method beyond 1000 Hz can also be taken as a side work. Finally, the entire simulation set up is done based on the TDD sytem. It would be also quite an interesting area to investigate the performance of the doppler estimations as well as the beamweight optimization in an FDD system.

Bibliography

[1] Katsuhiro Naito A.Doong Singhapan and Hideo Kobayashi. "Doppler frequencyspread estimation for OFDM systems in time varying fading channel", IEEE, 2012.

[2] Pierre Bertrand. "Frequency Offset Estimation in 3G LTE." IEEE, 2010.

[3] Yahong Rosa Zheng Chengshan Xiao and Norman C.Beaulieu. "Novel SumofSinusoids Simulation Models for Rayleigh and Rician Fading Channels" IEEE, 2006.

[4] Yong Soo Cho. MIMO-OFDM wireless communications with MATLAB. Wiley, 2010.

[5] Creative commons http://www.radio-electronics.com/info/cellulartelecomms/ lte-long-term-evolution/physical-logical-transport-channels.php.

[6] Creative commons. https://se.mathworks.com/help/comm/ref/comm. ofdmmodulator-class.html.

[7] Creative commons. http://whttps://commons.wikimedia.org/wiki/ File:SC-FDMA.svg.

[8] Stefan Parkvall Erik Dahlman and Johan Skold. 4G: LTE/LTE-Advanced for Mobile. Elsevier, 2014.

[9] EURASIP https://jwcn-eurasipjournals.springeropen.com/articles/ 10.1186/s13638-016-0670-9.

[10] Andrew Goldsmith. Wireless Communications. Cambridge University Press, 2005.

[11] Burcu Hanta. "SC-FDMA and LTE Uplink Physical Layer Design" IEEE, 2009.

[12] Harri Holma. LTE for UMTS : OFDMA and SC-FDMA based radio access. Wiley, 2009.

[13] Hassan Bajwaz Jawad Mirza Ataul Aziz Ikramy. "Maximum Doppler Shift Fre-

quency Estimation using Autocorrelation Function for MIMO OFDM Systems".
IEEE, 2010.

[14] G.Li J.Y.Hua D.H.Yuan and L.M.Meng. "Accurate estimation of Doppler shift
in mobile communications with high vehicle speed", International journal of
communications systems (2013).

[15] Paul D Yoo Omar Altrad Sami Muhaidat. "Doppler frequency estimation-based
handover algorithm for long-term evolution networks", IET Networks (2014).

[16] Theodore S. Rappaport. Wireless communications : principles and practice.
Prentice Hall PTR, 2002.

[17] Cihan Tepedelenlioglu and Georgios B. Giannakis. "On Velocity Estimation
and Correlation Properties of Narrow-Band Mobile Communication Channels",
IEEE (2013).

[18] math works. http://se.mathworks.com/help/lte/ug/fdd- and- tddduplex-
ing.html.

[19] Yang Liu Yinghui ZhangJing Gao. "MRT precoding in downlink multi-user
MIMO systems", EURASIP Journal on Wireless Communications and Net-
working (2016).

[20] Hyunsoo Cheon. "Frequency offset estimation for high speed users in E-UTRA
UPLINK", The 18th Annual IEEE International Symposium on Personal, In-
door and Mobile Radio Communications, 2007

[21] Yang Liu Yinghui ZhangJing Gao. "Time-Varying Doppler Frequency Offset
Estimation Method for LTE-TDD Uplink with Multi-user in HST Scenario",
Wireless Pers Commun (2015) 82:1127–1146

[22] Lei Song, Mugen Peng, Boxuan Lv, Mingmin Wang, and Hua Jiang. "Speed Es-
timation in Uplink Frequency Domain for Mobile OFDM Systems", IEEE/CIC
ICCC 2014 Symposium on Signal Processing for Communications